

# Effects of the thermal treatment on the luminescence of $\text{YVO}_4:\text{Er}^{3+}$ nanocrystals

S. GEORGESCU\*, O. TOMA, A. M. VOICULESCU

National Institute for Laser, Plasma and Radiation Physics, 409 Atomistilor Street, Măgurele, Jud. Ilfov, 077125, Romania

The modifications induced in  $\text{YVO}_4$  nanocrystals by the thermal treatments are observed and analyzed using  $\text{Er}^{3+}$  as a probe. These modifications are discussed in the frame of the Judd-Ofelt theory. The results are compared with the previous ones, obtained with  $\text{Eu}^{3+}$  as a probe.

(Received November 2, 2011; accepted November 23, 2011)

Keywords:  $\text{YVO}_4$ ,  $\text{Er}^{3+}$ , Nanocrystals, Luminescence, Judd-Ofelt

## 1. Introduction

$\text{YVO}_4:\text{Eu}$  is a strongly luminescent material which has been used as the red phosphor in cathode ray tubes for more than 20 years [1-3]. The crystalline  $\text{YVO}_4$  adopts the tetragonal structure (space group  $D_{4h}^{19} - I41/amd$  [4]) composed of  $\text{YO}_8$  dodecahedra (the point symmetry of  $\text{Y}^{3+}$  is  $D_{2d}$  [5]) and  $\text{VO}_4$  tetrahedra (symmetry  $D_{2d}$  [4]). The rare earth ions occupy the  $\text{Y}^{3+}$  site in  $\text{YVO}_4$  [5].

In a recent paper [6] we analyzed the effects of the thermal treatment on europium-doped  $\text{YVO}_4$  nanocrystals synthesized by direct precipitation technique using optical and Mössbauer spectroscopy. In this paper we analyze the effects of the thermal treatments on the erbium-doped  $\text{YVO}_4$  nanocrystals using optical spectroscopy.

## 2. Experimental

The  $\text{Y}_{0.95}\text{Er}_{0.05}\text{VO}_4$  nanocrystals were synthesized by direct precipitation reaction [7]. A mixture of two solutions ( $\text{Y}(\text{NO}_3)_3$  and  $\text{Er}(\text{NO}_3)_3$ ) was added to a solution of  $\text{NH}_4\text{VO}_3$  whose pH was adjusted to 12.5 with  $\text{NaOH}$ . The obtained colloid was heated at 60 °C for one hour under magnetic stirring. The nanocrystals were separated from the solution by filtering and then dried at 60 °C. The resulting powders were annealed at 400 °C, 600 °C, 900 °C and 1200 °C for four hours in air.

The luminescence spectra were recorded using a setup with a Xenon lamp with suitable filters as pumping source, a Jarrel-Ash monochromator (1 m) equipped with an S-20 photomultiplier, and a lock-in amplifier (SR 830) online with a PC. The luminescence signal was modulated with a SR 540 chopper.

## 3. Results and discussion

In Fig. 1 is shown part of the luminescence spectrum of  $\text{Er}^{3+}$  in  $\text{YVO}_4$  (transitions  ${}^2H_{11/2} \rightarrow {}^4I_{15/2}$  and  ${}^4S_{3/2} \rightarrow {}^4I_{15/2}$

${}^4I_{15/2}$ ). At room temperature the  ${}^2H_{11/2}$  and  ${}^4S_{3/2}$  are thermalized. In very simplified two level model (i.e. the crystal-field splitting of both  ${}^2H_{11/2}$  and  ${}^4S_{3/2}$  levels is neglected) the ratio of the populations  $N({}^2H_{11/2})/N({}^4S_{3/2}) = \exp(-\Delta E/k_B T)$ , where  $\Delta E$  is the energy difference between these two levels and  $k_B$  is the Boltzmann constant. Considering the difference between the gravity centers of  ${}^2H_{11/2}$  and  ${}^4S_{3/2}$  levels in  $\text{Er}:\text{YVO}_4$ ,  $\Delta E = 751 \text{ cm}^{-1}$  [8], it results  $\exp(-\Delta E/k_B T) = 0.0273$ . This explains the relative low intensity of the  ${}^2H_{11/2} \rightarrow {}^4I_{15/2}$  luminescence band in Fig. 1, though the radiative probability of this transition is rather large, as we shall see below.

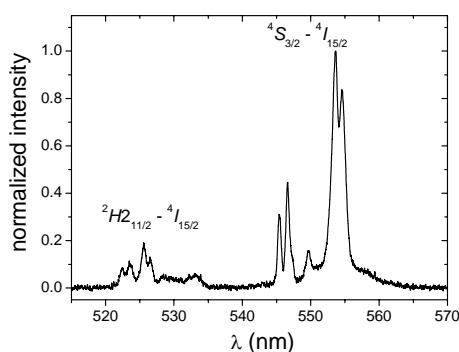


Fig. 1. Part of the luminescence spectrum of  $\text{Er}^{3+}$  in  $\text{YVO}_4$ . Only the  ${}^2H_{11/2} \rightarrow {}^4I_{15/2}$  and  ${}^4S_{3/2} \rightarrow {}^4I_{15/2}$  transitions are shown.

The majority of the observed optical transitions in lanthanide ions are induced electric-dipole transitions. In the frame of the Judd-Ofelt (JO) model [9, 10], the radiative transition probability for an electric-dipole  $f-f$  transition between the initial state  $||[\Psi'S'L']J'\rangle$  and the final state  $||[\Psi SL]J\rangle$  is given by

$$A^{ed}([\Psi'S'L']J', [\Psi SL]J) = \frac{64\pi^4 e^2}{3h(2J'+1)\tilde{\lambda}^3} \times n \left[ \frac{(n^2+2)^2}{9} \right] \sum_{k=2,4,6} \Omega_k \left| \langle [\Psi'S'L']J' \| U^{(k)} \| [\Psi SL]J \rangle \right|^2 \quad (1)$$

where  $\Omega_k$  are the three JO parameters and  $\left| \langle U^{(k)} \rangle \right|^2$  are the squares of the reduced matrix elements of the unitary operators  $U^{(k)}$ , in intermediary coupling and  $\tilde{\lambda}$  is the average wavelength of the transition. Their values for  $\text{Er}^{3+}$  for the transitions originating in  ${}^4S_{3/2}$  and  ${}^2H_{11/2}$  are given in Table. 1 (our calculations).

The emission transitions from  ${}^4S_{3/2}$  are pure electric dipole; those from  ${}^2H_{11/2}$  are *mainly* electric dipole. Neglecting the dispersion of the refractive index  $n$ , the contribution of the magnetic dipole transitions, and considering only the larger terms (i.e. those corresponding to  ${}^4S_{3/2} \rightarrow {}^4I_{15/2}$ ,  ${}^4S_{3/2} \rightarrow {}^4I_{13/2}$  and  ${}^2H_{11/2} \rightarrow {}^4I_{15/2}$ )

$$\frac{A^{ed}({}^2H_{11/2})}{A^{ed}({}^4S_{3/2})} \approx \frac{4}{12} \frac{(0.70836 \times \Omega_2 + 0.41081 \times \Omega_4) / 0.525^3}{\left( \frac{0.34563}{0.85^3} + \frac{0.21588}{0.55^3} \right) \Omega_6} \quad (2)$$

$$\approx 0.878 \times \Omega_2 / \Omega_6 + 0.509 \times \Omega_4 / \Omega_6$$

In Eq. (2), the average wavelengths are: 0.525  $\mu\text{m}$  corresponding to  ${}^2H_{11/2} \rightarrow {}^4I_{15/2}$ , 0.55  $\mu\text{m}$  – transition  ${}^2S_{3/2} \rightarrow {}^4I_{15/2}$ , and 0.85  $\mu\text{m}$  for  ${}^2S_{3/2} \rightarrow {}^4I_{13/2}$ .

Table 1. Squares of the reduced matrix elements of the unitary operators  $U^{(k)}$ . The largest matrix element entering Eq. (2) are emphasized.

Transition	$\left  \langle U^{(2)} \rangle \right ^2$	$\left  \langle U^{(4)} \rangle \right ^2$	$\left  \langle U^{(6)} \rangle \right ^2$
${}^2H_{11/2} \rightarrow {}^4S_{3/2}$	0	0.19626	0.01016
${}^2H_{11/2} \rightarrow {}^4F_{9/2}$	0.35118	0.01982	0.00396
${}^2H_{11/2} \rightarrow {}^4I_{9/2}$	0.20695	0.08618	0.31196
${}^2H_{11/2} \rightarrow {}^4I_{11/2}$	0.02991	0.17658	0.04331
${}^2H_{11/2} \rightarrow {}^4I_{13/2}$	0.02243	0.05893	0.05761
${}^2H_{11/2} \rightarrow {}^4I_{15/2}$	<b>0.70836</b>	<b>0.41081</b>	0.09488
${}^2S_{3/2} \rightarrow {}^4F_{9/2}$	0	0.00046	0.02756
${}^2S_{3/2} \rightarrow {}^4I_{9/2}$	0	0.08376	0.25443
${}^2S_{3/2} \rightarrow {}^4I_{11/2}$	0	0.00433	0.06939
${}^2S_{3/2} \rightarrow {}^4I_{13/2}$	0	0	<b>0.34563</b>
${}^2S_{3/2} \rightarrow {}^4I_{15/2}$	0	0	<b>0.21588</b>

The values of the JO parameters in bulk  $\text{Er:YVO}_4$  are  $\Omega_2 = 13.45 \times 10^{-20} \text{ cm}^2$ ,  $\Omega_4 = 2.23 \times 10^{-20} \text{ cm}^2$ , and  $\Omega_6 = 1.67 \times 10 \times 10^{-20} \text{ cm}^2$  [8]. Introducing these values in Eq. (2),  $A^{ed}({}^2H_{11/2}) / A^{ed}({}^4S_{3/2}) \approx 7.751$ .

The ratio  $R$  of the areas of the luminescence bands in Fig. 1 is proportional with the ratio of the radiative transitions probability multiplied with ratio of their populations:

$$R = \frac{\text{area}({}^2H_{11/2} \rightarrow {}^4I_{15/2})}{\text{area}({}^4S_{3/2} \rightarrow {}^4I_{15/2})} \propto \frac{A^{ed}({}^2H_{11/2} \rightarrow {}^4I_{15/2})}{A^{ed}({}^4S_{3/2} \rightarrow {}^4I_{15/2})} \exp(-\Delta E / k_B T) \quad (3)$$

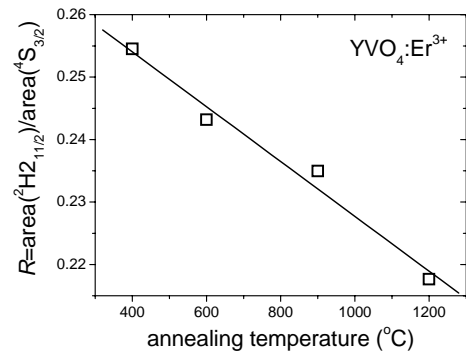


Fig. 2. The ratio  $R$  function of the annealing temperature. The straight line merely shows the decreasing of the parameter  $R$ .

In Fig. 2 is given the dependence of  $R$  of the annealing temperature. Increasing the annealing temperature, the ratio decreases, a similar behavior with the asymmetry ratio  $R_2$  in Ref. [6] (and with  $R_4$ , too). For an easier comparison, we reproduce separately the  $R_2$  (Fig. 3) and  $R_4$  (Fig. 4) dependences as measured for Eu-doped  $\text{YVO}_4$  [6].

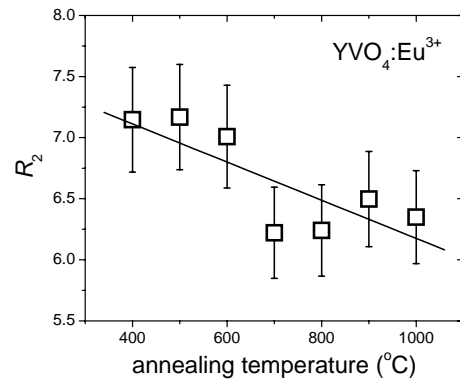


Fig. 3. The ratio  $R_2$  function of the annealing temperature. The straight line has the same meaning as in Fig. 2.

In  $\text{Eu}^{3+}$ -doped materials the ratio  $R_2$  (defined as the ratio between the area of the electric-dipole transition  ${}^5D_0 \rightarrow {}^7F_2$  and the area of the magnetic-dipole one,  ${}^5D_0 \rightarrow {}^7F_1$ )

is proportional with  $\Omega_2$  and ratio  $R_4$  (between the areas of  ${}^5D_0 \rightarrow {}^7F_4$  and  ${}^5D_0 \rightarrow {}^7F_1$ ) is proportional with  $\Omega_4$ .

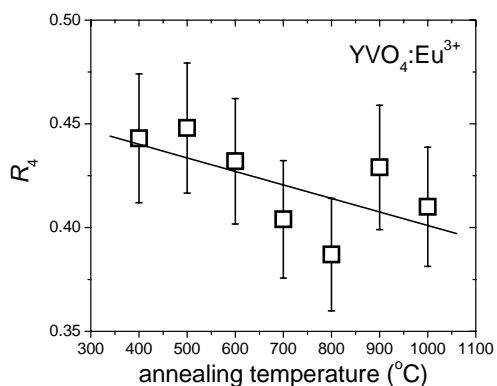


Fig. 4. The ratio  $R_4$  function of the annealing temperature. The straight line has the same meaning as in Fig. 2.

The experimental errors in Figs. 3 and 4 are larger than in Fig. 2, due to the relatively reduced area corresponding to the magnetic-dipole transition  ${}^5D_0 \rightarrow {}^7F_1$  in Eu<sup>3+</sup>:YVO<sub>4</sub>. Nevertheless, the decreasing of the  $R_2$  and  $R_4$  ratios is evident.

The JO parameters for bulk Eu<sup>3+</sup>:YVO<sub>4</sub> are:  $\Omega_2 = 7.49 \times 10^{-20}$  cm<sup>2</sup> and  $\Omega_4 = 0.47 \times 10^{-20}$  cm<sup>2</sup>, obtained from the fluorescence spectrum [19].  $\Omega_6$  was not determined due to the very reduced intensity of the  ${}^5D_0 \rightarrow {}^7F_6$  luminescence band. We note that the ratio of ours  $R_2$  and  $R_4$  is approximately equal with the ratio  $\Omega_2/\Omega_4$  from Ref. [19].

We observe that for erbium doped materials the term containing the ratio  $\Omega_2/\Omega_6$  is dominant in Eq. (2). Therefore, the reduction of the  $R$  in Fig. 2 is related mainly to the reduction of  $\Omega_2/\Omega_6$  ratio. An examination of the Figs. 3 and 4 shows that in the same temperature interval (400 – 1000°C) the dynamics of  $R_2$  and  $R_4$  (for Eu-doped YVO<sub>4</sub>) and of  $R$  (for Er-doped YVO<sub>4</sub>, Fig. 2, present paper) is approximately the same (for Er-doped sample, the value of  $R$  at 1000°C was obtained by linear interpolation). Since the dependence of  $\Omega_6$  of the annealing temperature in Eu-doped sample was not determined due to the very low intensity of the  ${}^5D_0 \rightarrow {}^7F_6$  transition, we can deduce its behavior comparing the results obtained for the  $\Omega_2$  and  $\Omega_4$  in Eu:YVO<sub>4</sub> and  $\Omega_2/\Omega_6$  in Er:YVO<sub>4</sub>. It results that the behavior of the ratio  $R$  in Er:YVO<sub>4</sub> is mainly given by  $\Omega_2$  and  $\Omega_6$  does not vary significantly.

#### 4. Conclusions

The ratio of the Judd-Ofelt parameters  $\Omega_2/\Omega_6$  is the dominant term in the evolution of the luminescence spectrum (transitions  ${}^2H_{21/2} \rightarrow {}^4I_{15/2}$  and  ${}^4S_{3/2} \rightarrow {}^4I_{15/2}$ ) of Er<sup>3+</sup> in YVO<sub>4</sub> nanocrystals as the result of the thermal treatments. In the frame of the experimental errors, this ratio has the same dynamics as  $\Omega_2$  in europium doped

YVO<sub>4</sub>. It results that Er<sup>3+</sup> could be used as a probe of the morphologic transformations induced by the thermal treatments.

#### Acknowledgement

This work was supported by the National Research Council (CNCS) in the frame of the Project (IDEI) ID 812 and by the Romanian National Center for Management of Programs (CNMP), project 12135/2008.

#### References

- [1] C. Brecher, H. Samelson, A. Lempicki, R. Riley, T. Peters, Phys. Rev., **155**, 178 (1967).
- [2] A. K Levine, F. C. Palilla, Appl. Phys. Lett., **5**, 118 (1964).
- [3] F. C. Palilla, A. K Levine, Applied Optics, **5**, 1467 (1966).
- [4] F. W. Kutzler, D. E. Ellis, D. J. Lam, B. W. Veal, A. P. Paulikas, A. T. Aldred, V. A. Gubanov, Phys. Rev. B **29**, 1008 (1984).
- [5] S. K. Misra, S. I. Andronenko, Phys. Rev. B, **64**, 094435 (2001).
- [6] A. M. Voiculescu, E. Cotoi, O. Toma, S. Georgescu, S. Constantinescu, I. Bibicu, Romanian Reports in Physics, **62**, 121 (2010).
- [7] Y. Li, G. Hong, J. Sol. State Chem., **178**, 645 (2005).
- [8] J. A. Capobianco, P. Kabro, F. S. Ermeneux, R. Moncorgé, M. Bettinelli, E. Cavalli, Chem. Phys. **214**, 239 (1997).
- [9] B. R. Judd, Phys. Rev. **127**, 750 (1962).
- [10] G. S. Ofelt, J. Chem. Phys. **37**, 511 (1962).
- [11] R. Reisfeld, E. Zigansky, M. Gaft, Mol. Phys. **102**, 1319 (2004).
- [12] G. Blasse, A. Bril, Philips Res. Repts. **21**, 368 (1966).
- [13] G. Blasse, A. Bril, W. C. Nieuwpoort, J. Phys. Chem. Sol. **27**, 1587 (1966).
- [14] W. C. Nieuwpoort, G. Blasse, Solid State Commun. **4**, 227 (1966).
- [15] J. A. Capobianco, P. P. Proulx, M. Bettinelli, F. Negrisolo, Phys. Rev. B **42**, 5936 (1990).
- [16] H. Takebe, K. Morinaga, T. Izumitani, J. Non-Crystalline Solids, **178**, 58 (1994).
- [17] E. W. J. L. Oomen, A. M. A. van Dongen, J. Non-Crystalline Solids, **111**, 205 (1989).
- [18] C. Görller-Walrand, K. Binnemans, in Handbook on the Physics and Chemistry of Rare Earths, Vol. **25** (Eds. K. A. Gschneider, Jr. and L. Eyring), Elsevier 1998, p. 229.
- [19] G. Pan, H. Song, Q. Dai, R. Qin, X. Bai, B. Dong, L. Fan, F. Wang, J. Appl. Phys. **104**, 084910 (2008).

Corresponding author: serban.georgescu@infplr.ro